Plasmin and chymotrypsin have distinct preferences for channel activating cleavage sites in the γ subunit of the human epithelial sodium channel

Silke Haerteis, Matteus Krappitz, Alexei Diakov, Annabel Krappitz, Robert Rauh, and Christoph Korbmacher

Institut für Zelluläre und Molekulare Physiologie, Friedrich-Alexander-Universität Erlangen-Nürnberg, 91054 Erlangen, Germany

Proteolytic activation of the epithelial sodium channel (ENaC) involves cleavage of its γ subunit in a critical region targeted by several proteases. Our aim was to identify cleavage sites in this region that are functionally important for activation of human ENaC by plasmin and chymotrypsin. Sequence alignment revealed a putative plasmin cleavage site in human γENaC (K189) that corresponds to a plasmin cleavage site (K194) in mouse γENaC. We mutated this site to alanine (K189A) and expressed human wild-type (wt) αβγENaC and $\alpha\beta\gamma_{K189A}$ENaC in *Xenopus laevis* oocytes. The γ_{K189A} mutation reduced but did not abolish activation of ENaC whole cell currents by plasmin. Mutating a putative prostasin site ($\gamma_{RKRK178AAAA}$) had no effect on the stimulatory response to plasmin. In contrast, a double mutation ($\gamma_{RKRK178AAAA;K189A}$) prevented the stimulatory effect of plasmin. We conclude that in addition to the preferential plasmin cleavage site K189, the putative prostasin cleavage site RKRK178 may serve as an alternative site for proteolytic channel activation by plasmin. Interestingly, the double mutation delayed but did not abolish ENaC activation by chymotrypsin. The time-dependent appearance of cleavage products at the cell surface nicely correlated with the stimulatory effect of chymotrypsin on ENaC currents in oocytes expressing wt or double mutant ENaC. Delayed proteolytic activation of the double mutant channel with a stepwise recruitment of so-called near-silent channels was confirmed in single-channel recordings from outside-out patches. Mutating two phenylalanines (FF174) in the vicinity of the prostasin cleavage site prevented proteolytic activation by chymotrypsin. This indicates that chymotrypsin preferentially cleaves at FF174. The close proximity of FF174 to the prostasin site may explain why mutating the prostasin site impedes channel activation by chymotrypsin. In conclusion, this study supports the concept that different proteases have distinct preferences for certain cleavage sites in γENaC, which may be relevant for tissue-specific proteolytic ENaC activation.

The Journal of General Physiology

INTRODUCTION

The epithelial sodium channel (ENaC) is localized in the apical membrane of epithelial cells and is the rate-limiting step for sodium absorption in several epithelial tissues including the aldosterone-sensitive distal nephron, respiratory epithelia, distal colon, and sweat and salivary ducts. The appropriate regulation of ENaC activity in the kidney is critically important for the maintenance of body sodium balance and hence for the long-term regulation of arterial blood pressure (Rossier and Schild, 2008; Loffing and Korbmacher, 2009).

ENaC is a member of the ENaC/degenerin family of ion channels that also includes the acid-sensing ion channel ASIC1. The recently published crystal structure of chicken ASIC1 suggests that ENaC is a heterotrimer composed of three homologous subunits: α, β, and γ (Canessa, 2007; Jasti et al., 2007; Stockand et al., 2008). Using atomic force microscopy, we recently provided morphological evidence for the heterotrimeric structure of ENaC (Stewart et al., 2011). In humans, an additional δ subunit exists that can functionally replace the α subunit in heterologous expression systems (Waldmann et al., 1995; Ji and Benos, 2004; Yamamura et al., 2004; Haerteis et al., 2009). Each subunit contains two transmembrane domains: a large extracellular domain, and short intracellular amino and carboxyl termini.

The tissue-specific regulation of ENaC by hormones and other factors is highly complex (Loffing and Korbmacher, 2009). It is an emerging concept that complex proteolytic processing is essential for channel activation under physiological and pathophysiological conditions (Kleyman et al., 2009; Rossier and Stutts, 2009; Svenningsen et al., 2011). Proteases contribute to ENaC regulation by cleaving specific sites in the extracellular loops of the α, γ, and δ subunits but not the β subunit (Adebamiro et al., 2007; Hughey et al., 2007;

S. Haerteis and M. Krappitz contributed equally to this paper.
Correspondence to Christoph Korbmacher: christoph.korbmacher@fau.de

Abbreviations used in this paper: ΔI_{ami}, amiloride-sensitive current; ENaC, epithelial sodium channel; wt, wild type.

The Rockefeller University Press $30.00
J. Gen. Physiol. Vol. 140 No. 4 375–389
www.jgp.org/cgi/doi/10.1085/jgp.201110763

Planès and Caughey, 2007; Diakov et al., 2008; Haerteis et al., 2009; Rossier and Stutts, 2009). Cleavage results in the release of inhibitory peptides and probably activates the channel by changing its conformation (Kleyman et al., 2009; Haerteis et al., 2012; Kashlan et al., 2012).

Proteolytic cleavage by the Golgi-associated convertase furin (Hughey et al., 2004) at three putative furin sites (two in α- and one in γENaC) is thought to be important for ENaC maturation in the biosynthetic pathway before the channel reaches the plasma membrane (Kleyman et al., 2009). The pivotal final step in proteolytic ENaC activation probably takes place at the plasma membrane where γENaC is cleaved by membrane-bound proteases and/or extracellular proteases in a region distal to the furin site (Adebamiro et al., 2007; Carattino et al., 2008; Diakov et al., 2008; Harris et al., 2008; Kota et al., 2012; Patel et al., 2012). Putative cleavage sites for prostasin (Bruns et al., 2007), plasmin (Passero et al., 2008), elastase (Adebamiro et al., 2007), and kallikrein (Patel et al., 2012) have been described in this region. In contrast, functionally relevant cleavage sites involved in ENaC activation by trypsin and chymotrypsin have not yet been identified. Interestingly, these prototypical serine proteases are commonly used as an experimental tool to achieve maximal proteolytic ENaC activation. These proteases may be expressed in epithelial cells (Firth et al., 1996; Koshikawa et al., 1998), but it is not yet known whether trypsin or chymotrypsin is relevant for ENaC activation in vivo.

According to the availability of proteases in tissues, distinct protease cleavage sites may be used in different tissues to cleave and activate ENaC. This may explain why different cleavage sites accumulate in this variable region in γENaC. However, the relevant proteases that cleave the γ subunit in this critical region under physiological conditions remain elusive and may differ in different tissues. Up to now, it is not known to what extent endogenous proteases constitutively activate ENaC in vivo under various physiological and pathological conditions. It has been reported that aldosterone-stimulated tissues show increased proteolytic cleavage (Ergonul et al., 2006; Frindt et al., 2008). This suggests that ENaC cleavage is associated with ENaC activation in the native tissue. Indeed, it has been demonstrated that trypsin can activate ENaC in microdissected mouse (Nesterov et al., 2008) and rat (Frindt et al., 2008) distal nephron.

Proteolytic activation of ENaC may also be involved in the pathogenesis of inflammatory diseases. One example is nephrotic syndrome, a kidney disease characterized by proteinuria, increased renal sodium absorption and edema formation. In patients with nephrotic syndrome, the defective glomerular filtration barrier allows the filtration of plasminogen into the tubular fluid (Vaziri et al., 1994). Filtered plasminogen is converted to the serine protease plasmin by tubular urokinase-type plasminogen activator (Piedagnel et al., 2006). Recently, we and others reported that plasmin can proteolytically activate ENaC heterologously expressed in *Xenopus laevis* oocytes (Passero et al., 2008; Svenningsen et al., 2009a). This suggests that ENaC activation by plasmin may contribute to renal sodium retention in nephrotic syndrome (Kleyman and Hughey, 2009; Passero et al., 2010; Svenningsen et al., 2012).

For mouse ENaC, a putative plasmin cleavage site in the γ subunit (K194) has been shown to be critical for channel activation by plasmin (Passero et al., 2008). In addition to a direct effect of plasmin, it has been suggested that low concentrations of plasmin may stimulate ENaC indirectly via activation of prostasin and subsequent channel cleavage at a putative prostasin cleavage site in the γ subunit (Svenningsen et al., 2009b). For human ENaC, the relevant cleavage sites for plasmin remain to be determined.

The aim of the present study was to identify cleavage sites in human γENaC that are functionally relevant for channel activation by plasmin and chymotrypsin.

MATERIALS AND METHODS

Chemicals

Plasmin from human plasma (ε-aminocaproic acid- and lysine-free) was obtained from Merck. Amiloride hydrochloride, trypsin (type I), and α-chymotrypsin (type II) from bovine pancreas were purchased from Sigma-Aldrich.

Plasmids

Full-length cDNAs for human wild-type (wt) α-, β-, and γENaC were provided by H. Cuppens (University of Leuven, Leuven, Belgium). They were subcloned into pcDNA3.1 vector, and linearized plasmids were used as templates for cRNA synthesis (mMessage mMachine; Ambion) using T7 as promotor. $\gamma_{FF174AA}$, $\gamma_{FF174AA;RKRK178AAAA;V182G;K189A;V193G}$, $\gamma_{RKRK178AAAA}$, γ_{K189A}, and $\gamma_{RKRK178AAAA;K189A}$ mutants were generated by site-directed mutagenesis (QuikChange Site-Directed Mutagenesis kit; Agilent Technologies), and sequences were confirmed (GATC Biotech). To minimize the risk of expression artifacts that may arise from differences in cRNA quality, cRNAs for wt and mutant ENaC were synthesized in parallel and the experiments were performed using at least two different batches of cRNA.

Isolation of oocytes and injection of cRNA

Oocytes were obtained from adult female *Xenopus laevis* in accordance with the principles of German legislation, with approval by the animal welfare officer for the University of Erlangen-Nürnberg, and under the governance of the state veterinary health inspectorate (permit no. 621–2531.32-05/02). Animals were anaesthetized in 0.2% MS222, and ovarian lobes were obtained through a small abdominal incision. After suture, the animals were allowed to recover fully in a separate tank before returning to the frog colony 1 d later. A minimum of 8 wk was obligatory before the next surgery on the same animal. Oocytes were isolated from the ovarian lobes by enzymatic digestion at 19°C for 3–4 h with 600–700 U/ml of type 2 collagenase from *Clostridium histolyticum* (CLS 2; Worthington) dissolved in a solution containing (in mM): 82.5 NaCl, 2 KCl, 1 $MgCl_2$, and 5 HEPES, pH 7.4 with NaOH. Defolliculated stage V–VI oocytes were injected (Nanoject II automatic injector; Drummond) with 0.2 ng cRNA per ENaC subunit, unless stated otherwise. The cRNAs

were dissolved in RNase-free water, and the total volume injected was 46 nl. Injected oocytes were stored at 19°C in low sodium solution (in mM: 87 NMDG-Cl, 9 NaCl, 2 KCl, 1.8 $CaCl_2$, 1 $MgCl_2$, and 5 HEPES, pH 7.4 with Tris) supplemented with 100 U/ml penicillin and 100 µg/ml streptomycin.

Two-electrode voltage clamp

Oocytes were routinely studied 2 d after injection using the two-electrode voltage clamp technique essentially as described previously (Haerteis et al., 2009; Rauh et al., 2010). Individual oocytes were placed in a small experimental chamber and constantly superfused with high sodium solution ND96 (in mM: 96 NaCl, 2 KCl, 1.8 $CaCl_2$, 1 $MgCl_2$, and 5 HEPES, pH 7.4 with Tris) supplemented with 2 µM amiloride (added from a 10-mM aqueous stock solution) at a rate of 2–3 ml/min at room temperature. Bath solution exchanges were controlled by a magnetic valve system (ALA BPS-8) in combination with a TIB14 interface (HEKA). Voltage clamp experiments were performed using an amplifier (OC-725C; Warner Instruments) interfaced via a LIH-1600 (HEKA) to a PC with PULSE 8.67 software (HEKA) for data acquisition and analysis. Oocytes were clamped at a holding potential of −60 mV. Downward current deflections in the current traces correspond to inward currents, i.e., movement of positive charge from the extracellular side into the cell. Amiloride-sensitive current (ΔI_{ami}) values were determined by washing out amiloride with amiloride-free ND96 and subtracting the whole cell currents measured in the presence of amiloride from the corresponding whole cell currents recorded in the absence of amiloride. For the determination of the stimulatory effect of plasmin or chymotrypsin, ΔI_{ami} was detected before and after exposure to the protease. To recover from the first measurement of ΔI_{ami}, the oocyte was placed for 5 min in ND96. Subsequently, the oocyte was transferred to 150 µl of protease-supplemented ND96 or ND96 alone as control and preincubated for a time as indicated.

Patch clamp

Single-channel recordings in outside-out membrane patches of ENaC-expressing oocytes were performed essentially as described previously (Diakov and Korbmacher, 2004; Diakov et al., 2008; Haerteis et al., 2009; Rauh et al., 2010) using conventional patch-clamp technique. Patch pipettes were pulled from borosilicate glass capillaries and had a tip diameter of ∼1–1.5 µm after fire polishing. Pipettes were filled with K-gluconate pipette solution (in mM: 90 K-gluconate, 5 NaCl, 2 Mg-ATP, 2 EGTA, and 10 mM HEPES, pH 7.28 with Tris). Seals were routinely formed in a low sodium NMDG-Cl bath solution (in mM: 95 NMDG-Cl, 1 NaCl, 4 KCl, 1 $MgCl_2$, 1 $CaCl_2$, and HEPES 10, pH 7.4 with Tris). In this bath solution, the pipette resistance averaged ∼7 MΩ. After seal formation, the bath solution was changed to a NaCl bath solution in which the NMDG-Cl was replaced by 95 mM NaCl. Membrane patches were voltage clamped at −70 mV, close to the calculated reversal potential of Cl^- ($E_{Cl} = -77.4$ mV) and K^+ ($E_K = -79.4$ mV) under our experimental conditions. Experiments were performed at room temperature (∼23°C). Single-channel current data were initially filtered at 500 Hz and sampled at 2 kHz. In multichannel patches, current traces were refiltered at 50 Hz to resolve the single-channel current amplitude (i). Channel activity was derived from binned current amplitude histograms as the product NP_O, where N is the number of channels and P_O is open probability (Korbmacher et al., 1995; Diakov and Korbmacher, 2004; Diakov et al., 2008; Krueger et al., 2009). The current level at which all channels are closed was determined in the presence of 2 µM amiloride. Continuous current traces of 30 s were selected from different experimental periods to analyze changes in NP_O.

Detection of ENaC cleavage products at the cell surface

Biotinylation experiments were performed essentially as described previously (Haerteis et al., 2009; Rauh et al., 2010), using 30 oocytes per group. All biotinylation steps were performed at 4°C. In some experiments, oocytes were preincubated for 5 min either in ND96 solution or in ND96 solution containing 10 µg/ml plasmin or 2 µg/ml chymotrypsin. After washing the oocytes three times with ND96 solution, they were incubated in the biotinylation buffer (in mM: 10 triethanolamine, 150 NaCl, and 2 $CaCl_2$, and 1 mg/ml EZ-link sulfo-NHS-SS-Biotin [Thermo Fisher Scientific], pH 9.5) for 15 min with gentle agitation. The biotinylation reaction was stopped by washing the oocytes twice for 5 min with quench buffer (in mM: 192 glycine and 25 Tris-Cl 25, pH 7.5). Subsequently, the oocytes were lysed by passing them through a 27-gauge needle in lysis buffer (in mM: 500 NaCl, 5 EDTA, and 50 Tris-Cl, pH 7.4) supplemented with protease inhibitor cocktail tablets (Complete Mini EDTA-free; Roche) according to the manufacturer's instructions. The lysates were centrifuged for 10 min at 1,500 *g*. Supernatants were transferred to 1.5-ml tubes (Eppendorf) and incubated with 0.5% Triton X-100 and 0.5% Igepal CA-630 for 20 min on ice. Biotinylated proteins were precipitated with 100 µl of Immunopure-immobilized Neutravidin beads (Thermo Fisher Scientific) washed with lysis buffer. After overnight incubation at 4°C with overhead rotation, the tubes were centrifuged for 3 min at 1,500 *g*. Supernatants were removed, and beads were washed three times with lysis buffer. 100 µl of 2× SDS-PAGE sample buffer (Rotiload 1; Roth) was added to the beads. Samples were boiled for 5 min at 95°C and centrifuged for 3 min at 20,000 *g* before loading the supernatants on a 10% SDS-PAGE. To detect γENaC cleavage fragments, we used a subunit-specific antibody against human γENaC at a dilution of 1:10,000 (Haerteis et al., 2009). Horseradish peroxidase–labeled secondary goat anti–rabbit antibody (Santa Cruz Biotechnology, Inc.) was used at a dilution of 1:50,000. Chemiluminescence signals were detected using ECL Plus (GE Healthcare). Densitometric analysis was performed with ImageJ 1.38x software (National Institutes of Health).

Statistical methods

Data are presented as mean ± SEM. N indicates the number of different batches of oocytes, and n is the number of individual oocytes studied. Statistical significance was assessed by using the appropriate version of Student's t test with GraphPad Prism 4.03 software (GraphPad Software) for Windows. Time constants (τ) were analyzed using PulseFit 8.0 software (HEKA).

Online supplemental material

The online supplemental material documents the baseline current levels of wt and the five mutant channels (Fig. S1), the data that plasmin failed to activate mouse ENaC with a mutated plasmin cleavage site (γ_{K194A}; Fig. S2), and the data demonstrating the concentration dependence of the stimulatory effect of plasmin on ENaC (Fig. S3). Figs. S1–S3 are available at http://www.jgp.org/cgi/content/full/jgp.201110763/DC1.

RESULTS

The stimulatory effect of plasmin is reduced but not abolished in oocytes expressing ENaC with a mutated putative plasmin site (γ_{K189A})

Mutating a putative plasmin cleavage site in mouse γENaC has been reported to prevent the stimulation of mouse ENaC by plasmin (Passero et al., 2008). To investigate whether a homologous putative plasmin cleavage site is present in human γENaC, we compared the protein sequence of mouse and human γENaC. This sequence comparison suggested a putative plasmin cleavage

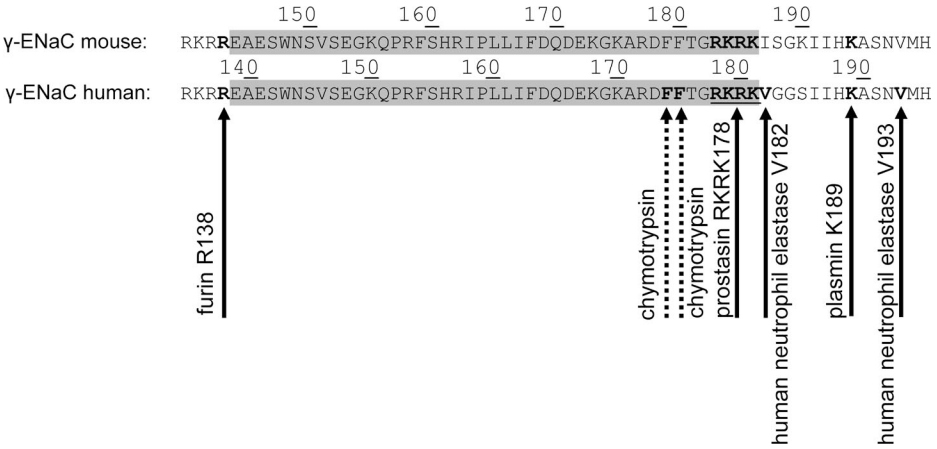

Figure 1. Sequence comparison of mouse γENaC (amino acids 140–200) and human γENaC (amino acids 135–195). The amino acid sequences of mouse γENaC and human γENaC are from the UniProt database (accession nos. Q9WU39 and P51170). The alignment demonstrates the high homology between the two species. The putative cleavage sites for furin (R138), chymotrypsin (FF174), prostasin (RKRK178), human neutrophil elastase (V182 and V193), and plasmin (K189) are indicated in bold and marked by an arrow.

site in human γENaC at position K189 (Fig. 1). To test the functional relevance of this cleavage site, we generated a γ_{K189A} mutant and expressed wt αβγENaC or mutant $\alpha\beta\gamma_{K189A}$ENaC in *Xenopus laevis* oocytes. With two-electrode voltage clamp, we measured amiloride-sensitive

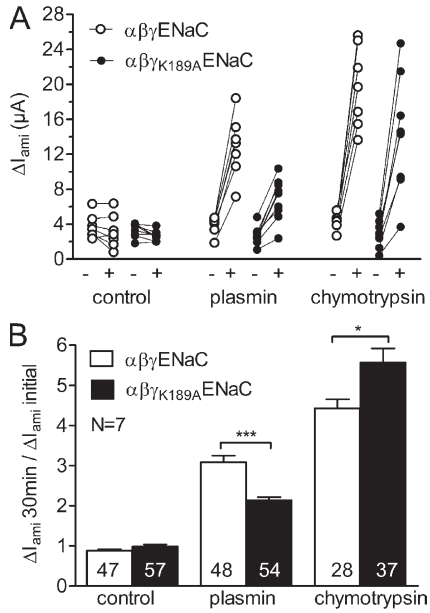

Figure 2. The stimulatory effect of plasmin is reduced but not abolished in oocytes expressing ENaC with a mutated putative plasmin site (γ_{K189A}). Oocytes expressing αβγ (open symbols) or $\alpha\beta\gamma_{K189A}$ENaC (closed symbols) were preincubated for 30 min in protease-free solution (control) or in solution containing either 10 μg/ml plasmin or 2 μg/ml chymotrypsin. Amiloride-sensitive whole cell currents (ΔI_{ami}) were determined before (−) and after (+) incubation. (A) Individual ΔI_{ami} values from a representative experiment using one batch of oocytes. Data points obtained from individual oocytes are connected by a line. (B) Summary of similar experiments as shown in A. Columns represent relative stimulatory effect on ΔI_{ami} calculated as the ratio of ΔI_{ami} measured after a 30-min preincubation (ΔI_{ami} 30 min) to the initial ΔI_{ami} (ΔI_{ami} initial) measured before incubation. Numbers inside the columns indicate the number of individual oocytes measured. *N* indicates the number of different batches of oocytes. *, $P < 0.05$; ***, $P < 0.001$; unpaired *t* test.

whole cell currents (ΔI_{ami}) in individual oocytes before and after 30-min exposure to 10 μg/ml plasmin. Basal ΔI_{ami} values of wt and γ_{K189A} mutant–expressing oocytes were of similar size (Figs. 2 A and S1 A), and exposure to plasmin activated both wt and mutant ENaC. However, the relative stimulatory effect of plasmin was significantly reduced by the γ_{K189A} mutation (Fig. 2 B). To test whether plasmin maximally activates ENaC under our experimental conditions, we also exposed wt and γ_{K189A} mutant ENaC–expressing oocytes for 30 min to 2 μg/ml chymotrypsin. Chymotrypsin is a prototypical serine protease known to fully activate ENaC (Chraïbi et al., 1998). Chymotrypsin stimulated ΔI_{ami} of wt ENaC–expressing oocytes more than plasmin (Fig. 2, A and B). This suggests that plasmin in the concentration used may not achieve its maximal stimulatory effect. However, with higher plasmin concentrations its stimulatory effect increases and approaches that of 2 μg/ml chymotrypsin (see Fig. S3). Interestingly, the γ_{K189A} mutation did not reduce but slightly enhanced the stimulatory effect of chymotrypsin on ΔI_{ami} (Fig. 2 B). In control experiments, a 30-min preincubation of wt and mutant ENaC–expressing oocytes in protease-free solution had a negligible effect on ENaC currents. In conclusion, the reduced stimulatory effect of plasmin on $\alpha\beta\gamma_{K189A}$ENaC suggests that γ_{K189} is a relevant plasmin cleavage site in human γENaC. However, the lack of a complete inhibition suggests that an additional cleavage site is involved in the activation of human ENaC by plasmin.

The stimulatory effect of plasmin is preserved in oocytes expressing ENaC with a mutated putative prostasin site ($\gamma_{RKRK178AAAA}$)

Recently, it has been reported that activation of rat ENaC by low concentrations of plasmin is mediated by prostasin (Svenningsen et al., 2009b). Thus, ENaC activation by plasmin may involve a prostasin cleavage site. Therefore, we studied the effect of plasmin on ENaC with a mutated putative prostasin cleavage site in the γ subunit ($\gamma_{RKRK178AAAA}$) (Fig. 3). We measured ΔI_{ami} in

individual oocytes before and after incubation of the oocytes for 30 min in 10 μg/ml plasmin. Basal ΔI_{ami} of wt αβγENaC and $\gamma_{RKRK178AAAA}$ mutant ENaC–expressing oocytes was not significantly different (Figs. 3 A and S1 B). Exposure to plasmin increased ΔI_{ami} of both wt and $\gamma_{RKRK178AAAA}$ mutant–expressing oocytes to a similar extent (Fig. 3 B). Interestingly, the stimulatory effect of 30-min chymotrypsin (2 μg/ml) exposure was slightly decreased in oocytes expressing $\gamma_{RKRK178AAAA}$ mutant ENaC (Fig. 3 B). This suggests that this site may contribute to proteolytic ENaC activation by chymotrypsin. Preincubation of wt and mutant ENaC–expressing oocytes for 30 min in protease-free solution had a negligible effect on ΔI_{ami} (Fig. 3 B). Collectively, these results suggest that the putative prostasin cleavage site per se is not required for the stimulatory effect of plasmin on human ENaC.

The stimulatory effect of plasmin on ENaC is abolished in oocytes expressing ENaC with a combined mutation of the plasmin and prostasin sites ($\alpha\beta\gamma_{RKRK178AAAA;K189A}$)

As described above, the stimulatory effect of plasmin on ENaC is significantly reduced in oocytes expressing ENaC with a mutated putative plasmin site but is preserved in oocytes expressing ENaC with a mutated putative prostasin site. Next, we generated a γENaC construct with the double mutation $\gamma_{RKRK178AAAA;K189A}$ and expressed wt αβγ or mutant $\alpha\beta\gamma_{RKRK178AAAA;K189A}$ENaC in oocytes. ΔI_{ami} of individual oocytes was measured before and after a 30-min preincubation in 10 μg/ml plasmin (Fig. 4). Similar to the two single mutations (Figs. 2 and 3), the $\gamma_{RKRK178AAAA;K189A}$ mutation had no significant effect on basal ΔI_{ami} (Figs. 4 A and S1 C). However, the stimulatory effect of plasmin on ENaC was abolished in oocytes expressing ENaC with mutated plasmin and prostasin

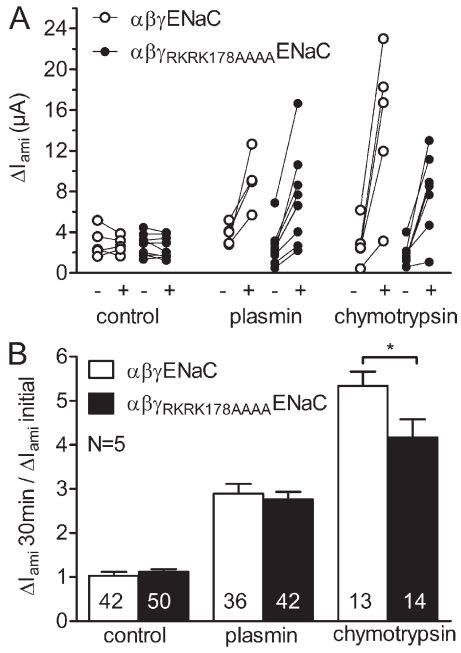

Figure 3. The stimulatory effect of plasmin is preserved in oocytes expressing ENaC with a mutated putative prostasin site ($\gamma_{RKRK178AAAA}$). Oocytes expressing αβγ (open symbols) or $\alpha\beta\gamma_{RKRK178AAAA}$ENaC (closed symbols) were preincubated for 30 min in protease-free solution (control) or in solution containing either 10 μg/ml plasmin or 2 μg/ml chymotrypsin. Amiloride-sensitive whole cell currents (ΔI_{ami}) were determined before (−) and after (+) incubation. (A) Individual ΔI_{ami} values from a representative experiment using one batch of oocytes. Data points obtained from individual oocytes are connected by a line. (B) Summary of similar experiments as shown in A. Columns represent relative stimulatory effect on ΔI_{ami} calculated as the ratio of ΔI_{ami} measured after a 30-min preincubation (ΔI_{ami} 30 min) to the initial ΔI_{ami} (ΔI_{ami} initial) measured before incubation. Numbers inside the columns indicate the number of individual oocytes measured. *N* indicates the number of different batches of oocytes. *, $P < 0.05$; unpaired *t* test.

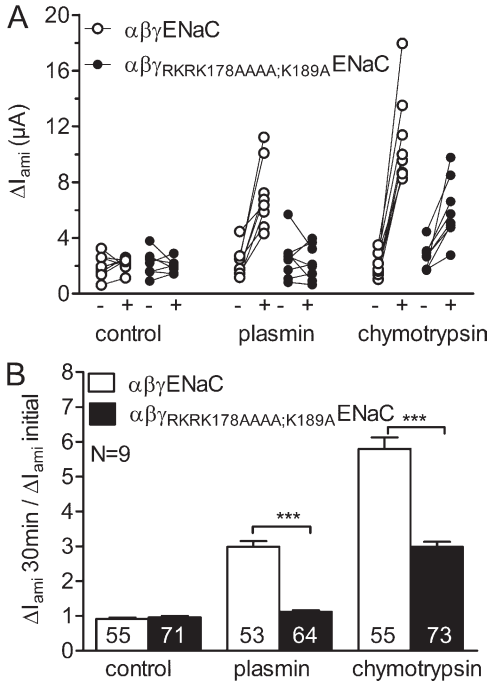

Figure 4. The stimulatory effect of plasmin on ENaC is abolished in oocytes expressing ENaC with a combined mutation of the plasmin and prostasin sites ($\alpha\beta\gamma_{RKRK178AAAA;K189A}$). Oocytes expressing αβγ (open symbols) or $\alpha\beta\gamma_{RKRK178AAAA;K189A}$ENaC (closed symbols) were preincubated for 30 min in protease-free solution (control) or in solution containing either 10 μg/ml plasmin or 2 μg/ml chymotrypsin. Amiloride-sensitive whole cell currents (ΔI_{ami}) were determined before (−) and after (+) incubation. (A) Individual ΔI_{ami} values from a representative experiment using one batch of oocytes. Data points obtained from individual oocytes are connected by a line. (B) Summary of similar experiments as shown in A. Columns represent relative stimulatory effect on ΔI_{ami} calculated as the ratio of ΔI_{ami} measured after a 30-min preincubation (ΔI_{ami} 30 min) to the initial ΔI_{ami} (ΔI_{ami} initial) measured before incubation. Numbers inside the columns indicate the number of individual oocytes measured. *N* indicates the number of different batches of oocytes. ***, $P < 0.001$; unpaired *t* test.

sites ($\alpha\beta\gamma_{RKRK178AAAA;K189A}$) (Fig. 4 B). This finding indicates that the double mutation prevents channel activation by plasmin. To test whether the double mutation also alters ENaC activation by chymotrypsin, we exposed wt and $\gamma_{RKRK178AAAA;K189A}$ mutant ENaC–expressing oocytes for 30 min to 2 µg/ml chymotrypsin. Interestingly, the double mutation significantly reduced but did not abolish the stimulatory effect of chymotrypsin on ENaC (Fig. 4 B). We conclude that in addition to the putative plasmin site (γ_{K189}), the putative prostasin cleavage site ($\gamma_{RKRK178}$) can serve as a cleavage site for plasmin to activate human ENaC. Moreover, the double mutation also affects proteolytic channel activation by chymotrypsin.

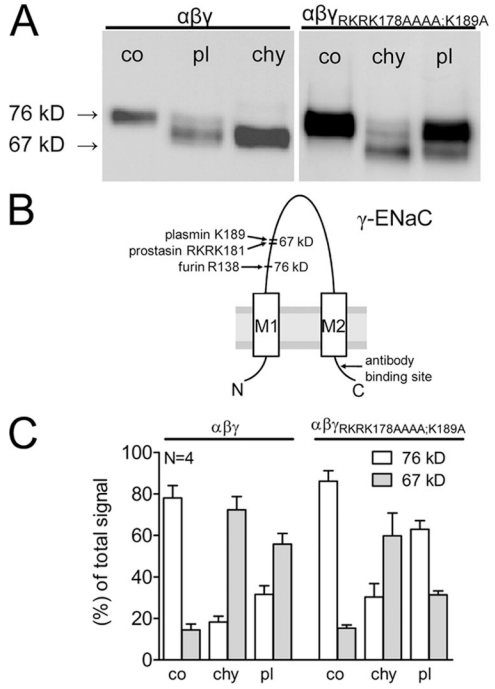

Figure 5. Mutating both the plasmin and the prostasin cleavage site ($\alpha\beta\gamma_{RKRK178AAAA;K189A}$) reduces proteolytic cleavage of γENaC at the cell surface. Oocytes were treated as described in the legend of Fig. 4. In parallel to the detection of ΔI_{ami} (shown in Fig. 4), expression of biotinylated γENaC at the cell surface was analyzed by SDS-PAGE. γENaC was detected with an antibody against the C terminus of human γENaC. Oocytes expressing αβγ or $\alpha\beta\gamma_{RKRK178AAAA;K189A}$ENaC were preincubated for 30 min in protease-free solution (control [co]) or in solution containing either 10 µg/ml plasmin (pl) or 2 µg/ml chymotrypsin (chy). (A) Representative Western blots from oocytes expressing αβγ or $\alpha\beta\gamma_{RKRK178AAAA;K189A}$ ENaC. (B) Model of the γENaC subunit showing cleavage sites for proteolytic activation and the binding site of the antibody used. (C) Densitometric analysis of similar Western blots as shown in A. For each lane, the signals detected in the regions of 76 kD (open columns) and 67 kD (gray columns) were determined and normalized to the sum of the total signal detected. *N* indicates the number of different batches of oocytes.

Mutating both the plasmin and the prostasin cleavage site ($\alpha\beta\gamma_{RKRK178AAAA;K189A}$) reduces proteolytic cleavage of ENaC at the cell surface

Proteolytic activation of γENaC is associated with the appearance of different cleavage products. For rat and mouse γENaC, it has previously been shown that in addition to a full-length 87-kD band, a cleavage product of ~76 kD appears when γENaC is coexpressed together with α- and βENaC (Hughey et al., 2004; Bruns et al., 2007; Harris et al., 2007, 2008). This cleavage product results from cleavage of γENaC by endogenous proteases like furin at the so-called furin cleavage site. An additional 67-kD band can be detected resulting from cleavage in a region distal to the furin site. This second cleavage step is critical for activation of membrane-resident ENaC and is thought to be mediated by extracellular proteases. Therefore, this 67-kD band is likely to represent the pool of activated ENaC (Bruns et al., 2007; Diakov et al., 2008). ENaC activation by plasmin or chymotrypsin should result in the appearance of the 67-kD fragment. Mutating relevant cleavage sites should diminish or prevent the appearance of the 67-kD band. To test this idea, we treated wt αβγENaC and double mutant $\alpha\beta\gamma_{RKRK178AAAA;K189A}$ENaC–expressing oocytes for 30 min with 2 µg/ml chymotrypsin or 10 µg/ml plasmin and detected cell surface–expressed γENaC cleavage fragments by Western blot with an antibody directed against the C terminus of γENaC (Fig. 5, A and B). As shown in Fig. 5 (A and C), the predominant γENaC fragment detected at the cell surface of untreated wt ENaC–expressing control oocytes had a molecular mass of ~76 kD. The signal for full-length γENaC (87 kD) usually was not detectable, which is in agreement with previously reported data (Harris et al., 2007, 2008). In noninjected oocytes, γENaC-specific signals were absent (not depicted). Exposure to plasmin was associated with the appearance of a 67-kD band and a reduction of the 76-kD band. The occurrence of the 67-kD cleavage product indicates cleavage of the γ subunit by plasmin at an additional site distal to the furin cleavage site. Plasmin resulted in a partial conversion of the 76-kD band into a 67-kD band in four out of eight experiments and in a complete conversion in the remaining experiments. In contrast, exposure to chymotrypsin caused a complete band shift from 76 to 67 kD in all experiments (Fig. 5, A and C). These findings are in good agreement with the observation that on average, chymotrypsin had a larger stimulatory effect on wt ENaC than plasmin (Figs. 2–4).

Similar to the finding in untreated wt ENaC–expressing oocytes, the 76-kD band was the only detectable biotinylated γENaC cleavage product in untreated double mutant ENaC–expressing oocytes (Fig. 5, A and C). Importantly, exposure of double mutant ENaC–expressing oocytes to plasmin only produced a faint band at 67 kD, whereas the predominant band remained at 76 kD

(Fig. 5, A and C). This supports the hypothesis that the double mutation prevents cleavage of γENaC by plasmin at the plasma membrane. In contrast, chymotrypsin treatment of double mutant ENaC–expressing oocytes resulted in the appearance of a substantial 67-kD band. Consistent with the reduced stimulatory effect of chymotrypsin on ENaC currents, the conversion of the 76-kD band into the 67-kD band was less complete in oocytes expressing the double mutant channel than in those expressing wt ENaC (Fig. 5, A and C). Thus, our results demonstrate that the disappearance of the 76-kD γENaC fragment and the appearance of the 67-kD γENaC fragment nicely correlate with the stimulatory effects of plasmin and chymotrypsin on ENaC-mediated whole cell currents. Hence, cleavage of the γENaC subunit in the prostasin/plasmin regions seems to convert the channel into an active channel.

Activation with chymotrypsin after activation with plasmin

The findings of partial γENaC cleavage and partial current activation of wt ENaC by plasmin suggest that after ENaC activation with plasmin, an additional activation with chymotrypsin should be possible. To investigate this, we preincubated wt αβγENaC and double mutant $\alpha\beta\gamma_{RKRK178AAAA;K189A}$ENaC–expressing oocytes for 30 min in plasmin or chymotrypsin and subsequently tested the acute effect of chymotrypsin on oocyte whole cell currents. In Fig. 6 (A–C), three representative whole cell current traces are shown that were obtained from oocytes expressing either wt αβγENaC (Fig. 6, A and B) or $\alpha\beta\gamma_{RKRK178AAAA;K189A}$ENaC (Fig. 6 C). The recordings were started in the presence of 2 μM amiloride. Washout of amiloride revealed a sizeable inward current component (ΔI_{ami}) that corresponds to the ENaC-mediated sodium current. In αβγENaC-expressing oocytes preincubated in chymotrypsin for 30 min, a subsequent exposure to chymotrypsin resulted in a minor additional increase (<10%) of ΔI_{ami} (Fig. 6, A and D). This is not surprising, as a 30-min preincubation with chymotrypsin in the concentration used can be expected to activate the majority of channels present at the plasma membrane. Thus, a second exposure to chymotrypsin is likely to have little additional stimulatory effect except on a few noncleaved channels that may be inserted into the plasma membrane in the short time period between the end of the preexposure time and the second chymotrypsin application (usually <3 min). In contrast, in αβγENaC-expressing oocytes preincubated in plasmin for 30 min, a subsequent exposure to chymotrypsin caused a sizeable increase (∼30%) of ΔI_{ami} (Fig. 6, B and D). This indicates that proteolytic activation of ENaC by a 30-min preincubation in plasmin is incomplete. This is consistent with the finding that preincubation of αβγENaC-expressing oocytes with chymotrypsin has a larger stimulatory effect on ENaC currents (Figs. 2–4) and cleavage (Fig. 5) than preincubation with plasmin. Importantly, the application of chymotrypsin to $\alpha\beta\gamma_{RKRK178AAAA;K189A}$ENaC-expressing oocytes preincubated in plasmin (Fig. 6 C) resulted in an increase of ΔI_{ami} that was slower (Fig. 6 C) but eventually reached a higher level (∼60%) than that observed in αβγENaC-expressing oocytes preincubated in plasmin (Fig. 6 D). This finding indicates that the double mutation not only prevents channel activation by plasmin but also affects channel activation by chymotrypsin.

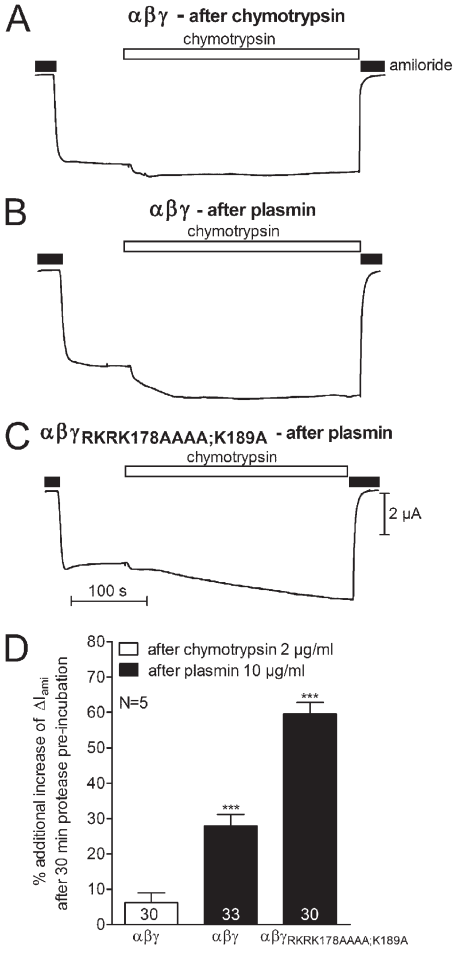

Figure 6. Activation with chymotrypsin after activation with plasmin. Representative whole cell current traces from oocytes expressing αβγ (A and B) or $\alpha\beta\gamma_{RKRK178AAAA;K189A}$ (C) ENaC after a 30-min preincubation in a solution containing 2 μg/ml chymotrypsin (A) or 10 μg/ml plasmin (B and C). 2 μM amiloride and 2 μg/ml chymotrypsin were present in the bath solution, as indicated by closed and open bars, respectively. (D) Average data obtained from five different batches of oocytes. Columns represent additional increase of ΔI_{ami} calculated as the ratio of ΔI_{ami} after superfusion with chymotrypsin to ΔI_{ami} after a 30-min preincubation in chymotrypsin (open column) or plasmin (closed columns). Numbers inside the columns indicate the number of individual oocytes analyzed. *N* indicates the number of different batches of oocytes. ***, $P < 0.001$; unpaired *t* test.

Mutating both the plasmin and the prostasin cleavage site delays proteolytic ENaC activation by chymotrypsin

To further investigate the effect of the $\gamma_{RKRK178AAAA;K189A}$ mutation on channel activation by chymotrypsin, we treated wt αβγENaC and double mutant $\alpha\beta\gamma_{RKRK178AAAA;K189A}$ENaC–expressing oocytes for 5, 30, and 60 min with chymotrypsin and detected the effects on ΔI_{ami} and on surface expression of γENaC in parallel. Fig. 7 A presents the relative stimulatory effect on ENaC currents after different exposure times to chymotrypsin. ΔI_{ami} of wt ENaC–expressing oocytes was already approximately fourfold activated after 5 min and fully activated (approximately sixfold) after 30 min. In contrast, a 5-min chymotrypsin exposure of mutant ENaC–expressing oocytes had a minor stimulatory effect on ΔI_{ami}, and approximately fourfold activation was reached only after a 30-min exposure. After a 60-min exposure to chymotrypsin, ΔI_{ami} in double mutant ENaC–expressing oocytes was still below that in wt ENaC–expressing oocytes.

Detection of γENaC at the cell surface in untreated wt ENaC–expressing control oocytes revealed a predominant 76-kD band (Fig. 7, B and C), which confirms the results shown above. A 5-min exposure to chymotrypsin was associated with the appearance of a 67-kD band and a decrease of the 76-kD signal (Fig. 7, B and C). After a 30-min chymotrypsin exposure, the 67-kD band was further increased to a maximal level and the 76-kD band had nearly disappeared (Fig. 7, B and C). These results indicate that the appearance of the 67-kD band correlates with the observed current increase over time (Fig. 7 A).

In untreated double mutant ENaC–expressing oocytes, the 76-kD band was also the predominant band (Fig. 7, D and E). Importantly, after a 5-min exposure to chymotrypsin, the 76-kD band remained predominant without substantial appearance of a 67-kD band (Fig. 7, D and E). After 30 min of chymotrypsin treatment, a strong 67-kD band appeared with a remaining 76-kD band (Fig. 7, D and E). After 60 min of chymotrypsin exposure, the 67-kD band became the predominant band and the 76-kD band almost disappeared (Fig. 7, D and E). Thus, in mutant ENaC–expressing oocytes, the delayed appearance of the 67-kD band nicely correlated with the delayed onset of proteolytic current activation.

Time constant of proteolytic ENaC activation by chymotrypsin is significantly increased in the $\alpha\beta\gamma_{RKRK178AAAA}$ and the $\alpha\beta\gamma_{RKRK178AAAA;K189A}$ mutant channel

To further investigate the effect of mutating the plasmin and the prostasin cleavage sites on the time course of proteolytic current activation, we continuously monitored the stimulatory effect of chymotrypsin on ENaC-mediated whole cell currents and determined a time constant (τ) for current activation. Fig. 8 (A–D) shows four representative current traces of oocytes expressing

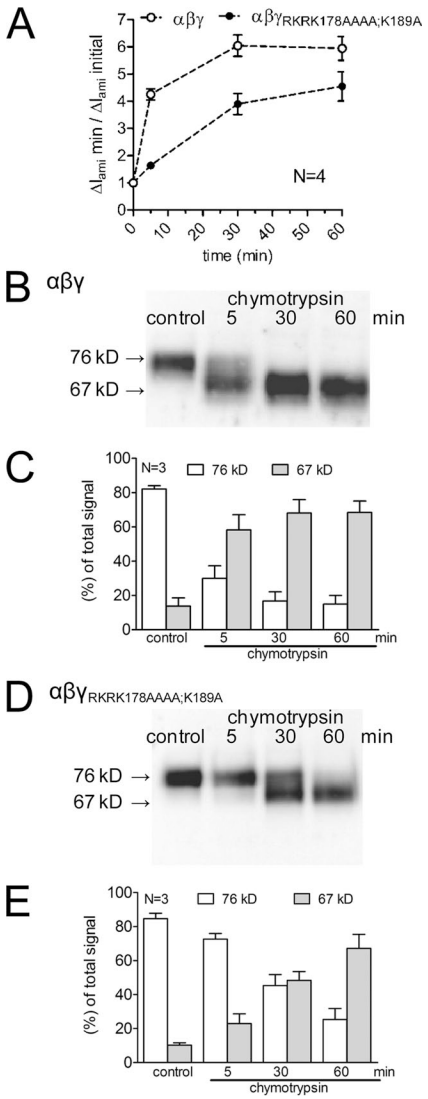

Figure 7. Mutating both the plasmin and the prostasin cleavage site delays proteolytic ENaC activation by chymotrypsin. Oocytes expressing αβγ (open symbols) or $\alpha\beta\gamma_{RKRK178AAAA;K189A}$ENaC (closed symbols) were preincubated for 30 min in protease-free solution (control) or for 5, 30, or 60 min in a solution containing 2 μg/ml chymotrypsin. Amiloride-sensitive whole cell currents (ΔI_{ami}) were determined before (−) and after (+) incubation. In parallel to the detection of ΔI_{ami}, expression of biotinylated γENaC at the cell surface was analyzed by SDS-PAGE. γENaC was detected with an antibody against the C terminus of human γENaC. (A) Circles represent the ratio of ΔI_{ami} measured after a 5-, 30-, or 60-min preincubation (ΔI_{ami} min) to the initial ΔI_{ami} (ΔI_{ami} initial) measured before incubation. Each data point represents the mean ΔI_{ami} measured in 22–24 individual oocytes of four different batches. (B and D) γENaC was detected with an antibody against the C terminus of human γENaC. Representative Western blot from one batch of oocytes. In noninjected oocytes, γENaC-specific signals were absent (not depicted). (C and E) Densitometric analysis of three Western blots similar to those shown in B or D. For each lane, the signals detected in the regions of 76 kD (open columns) and 67 kD (gray columns) were determined and normalized to the sum of the total signal detected. *N* indicates the number of different batches of oocytes.

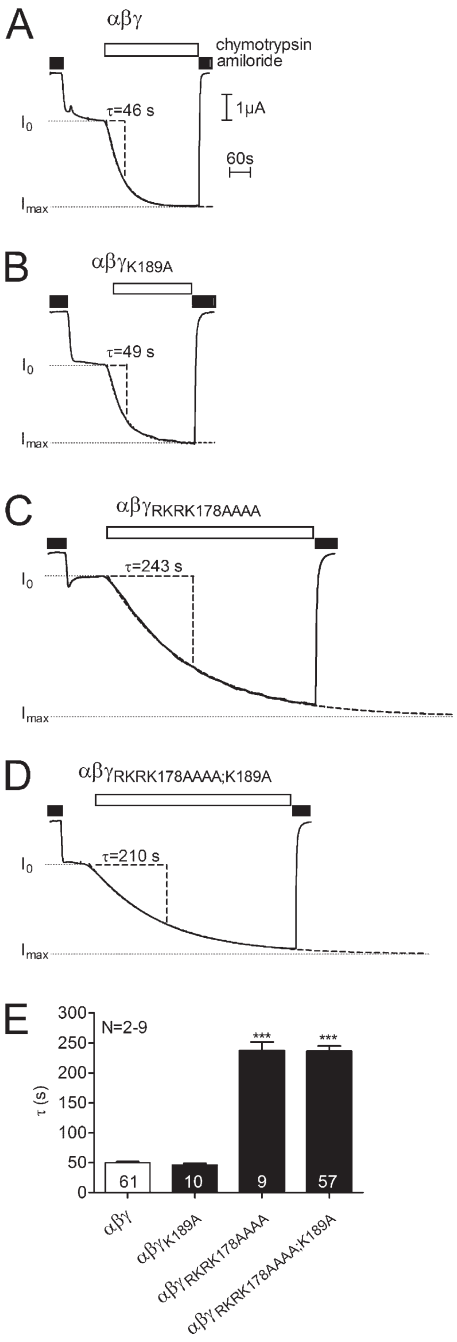

Figure 8. Time constant of proteolytic ENaC activation by chymotrypsin is significantly increased in the $\alpha\beta\gamma_{RKRK178AAAA}$ and the $\alpha\beta\gamma_{RKRK178AAAA;K189A}$ mutant channel. Representative whole cell current traces from oocytes expressing αβγ (A), $\alpha\beta\gamma_{K189A}$ (B), $\alpha\beta\gamma_{RKRK178AAAA}$ (C), and $\alpha\beta\gamma_{RKRK178AAAA;K189A}$ (D) ENaC. 2 μM amiloride and 2 μg/ml chymotrypsin were present in the bath solution, as indicated by closed and open bars, respectively. Values for the time constant (τ) of proteolytic current activation were estimated by fitting individual current traces with an exponential function $I(t) = I_0 + (I_{max} - I_0) \cdot (1 - e^{(-t/\tau)})$. Fitted curves are shown by broken lines superimposed on the representative current traces. The baseline current level before the application of chymotrypsin (I_0) and the extrapolated current maximum (I_{max}) are indicated by dotted lines. The length of the time constant (τ) is indicated. (E) Average τ obtained from up to nine different batches of oocytes. Numbers inside the columns indicate the number of individual oocytes analyzed. *N* indicates the number of different batches of oocytes. ***, $P < 0.001$; unpaired *t* test.

either wt αβγENaC (Fig. 8 A), $\alpha\beta\gamma_{K189A}$ (Fig. 8 B), $\alpha\beta\gamma_{RKRK178AAAA}$ (Fig. 8 C), or $\alpha\beta\gamma_{RKRK178AAAA;K189A}$ENaC (Fig. 8 D). The time courses of current activation caused by chymotrypsin showed a similar τ for wt and $\alpha\beta\gamma_{K189A}$ENaC-expressing oocytes (Fig. 8 E). However, compared with wt ENaC, τ of $\alpha\beta\gamma_{RKRK178AAAA}$ and $\alpha\beta\gamma_{RKRK178AAAA;K189A}$ENaC-expressing oocytes was approximately sixfold and approximately fivefold larger, respectively. These results demonstrate that mutating the putative plasmin cleavage site alone has no significant effect on the time course of ENaC activation by chymotrypsin, whereas inactivation of the putative prostasin cleavage site causes a delay, independent of the putative plasmin cleavage site. This is in good agreement with the finding that activation of $\gamma_{RKRK178AAAA}$ mutant channel by chymotrypsin after 30 min is slightly reduced compared with wt ENaC (Fig. 3). The finding that the time course of current activation by chymotrypsin can be fitted with a single-exponential function is consistent with the concept that a single cleavage event, i.e., proteolytic cleavage of γENaC in a critical region, is the rate-limiting final step of proteolytic channel activation.

Delayed proteolytic activation of near-silent channels in outside-out patches from oocytes expressing the $\alpha\beta\gamma_{RKRK178AAAA;K189A}$ mutant channel

ENaC populations with different P_O values exist in the plasma membrane (Firsov et al., 1996; Rossier, 2002), including a pool of so-called near-silent channels (Caldwell et al., 2004, 2005) that can be acutely activated by extracellular proteases (Diakov et al., 2008; Rauh et al., 2010). We hypothesized that the delayed stimulatory effect of chymotrypsin on ENaC whole cell currents may be related to a delayed onset of recruitment of near-silent channels in oocytes expressing the double mutant channel. To test this possibility, we investigated the effect of chymotrypsin on αβγ wt and $\alpha\beta\gamma_{RKRK178AAAA;K189A}$ mutant channels in outside-out membrane patches of oocytes. Fig. 9 (A and B) shows representative single-channel recordings from wt and double mutant ENaC–containing patches. Fig. 9 C summarizes NP_O values taken from different time intervals of individual current traces. In the recording shown in Fig. 9 A (top trace), a single-channel activity with up to eight apparent channel levels was observed. About 2 min after chymotrypsin application, at least 21 wt ENaC channels were active in the patch, consistent with the recruitment of additional channels (Caldwell et al., 2004, 2005; Diakov et al., 2008; Rauh et al., 2010). After chymotrypsin treatment, the single-channel current amplitude of wt ENaC was

unchanged at −0.38 pA. However, chymotrypsin treatment increased the NP_O of wt ENaC from 3.5 before to 17.9 after application of chymotrypsin. On average, exposure to chymotrypsin increased NP_O of wt ENaC from 1.6 before to 7.0 (n = 7) after a 12-min application of chymotrypsin. The recordings in patches of $\gamma_{RKRK178AAAA;K189A}$ mutant–expressing oocytes revealed that the double mutation had no apparent effect on the single-channel properties. In particular, the single-channel amplitude of the double mutant at a holding potential of −70 mV was not significantly different from that of wt ENaC (Fig. 9, A, bottom trace, and B). Importantly, in patches from oocytes expressing the double mutant, we did not observe an increase in the number of apparent channel levels within the first 2–3 min after application of chymotrypsin. Exposure to chymotrypsin increased NP_O of double mutant ENaC from 2.2 before to 3.2 after the application of chymotrypsin (Fig. 9 A, bottom trace). On average, exposure to chymotrypsin increased NP_O of double mutant ENaC from 1.8 before to 6.7 (n = 6) after a 12-min application of chymotrypsin. Interestingly, Fig. 9 (B and C) demonstrates that in patches that were stable enough to perform sufficiently long recordings, a delayed activation of near-silent channels could also be observed in double mutant ENaC–containing patches. This is consistent with the delayed stimulatory effect of chymotrypsin on double mutant ENaC observed in our whole oocyte current recordings (Figs. 7 A and 8 D). Our patch-clamp experiments demonstrate that proteolytic activation of both wt and double mutant ENaC by chymotrypsin is caused by a stepwise recruitment of so-called near-silent channels. Except for a slower time course, the electrophysiological pattern of proteolytic activation of the double mutant channel was similar to that of wt ENaC.

Mutating two phenylalanine residues (γFF174) adjacent to the prostasin cleavage site prevents proteolytic activation of ENaC by chymotrypsin

Interestingly, adjacent to the prostasin cleavage site there are two phenylalanines (γF174 and γF175) that represent putative cleavage sites for chymotrypsin (chymotrypsin preferentially cleaves after phenylalanine, tyrosine, and tryptophan). To investigate the role of these two phenylalanines in ENaC activation by chymotrypsin, we compared the effect of chymotrypsin on wt and $\alpha\beta\gamma_{FF174AA}$ mutant ENaC (Fig. 10). We found that the $\gamma_{FF174AA}$ mutation largely reduced the stimulatory effect

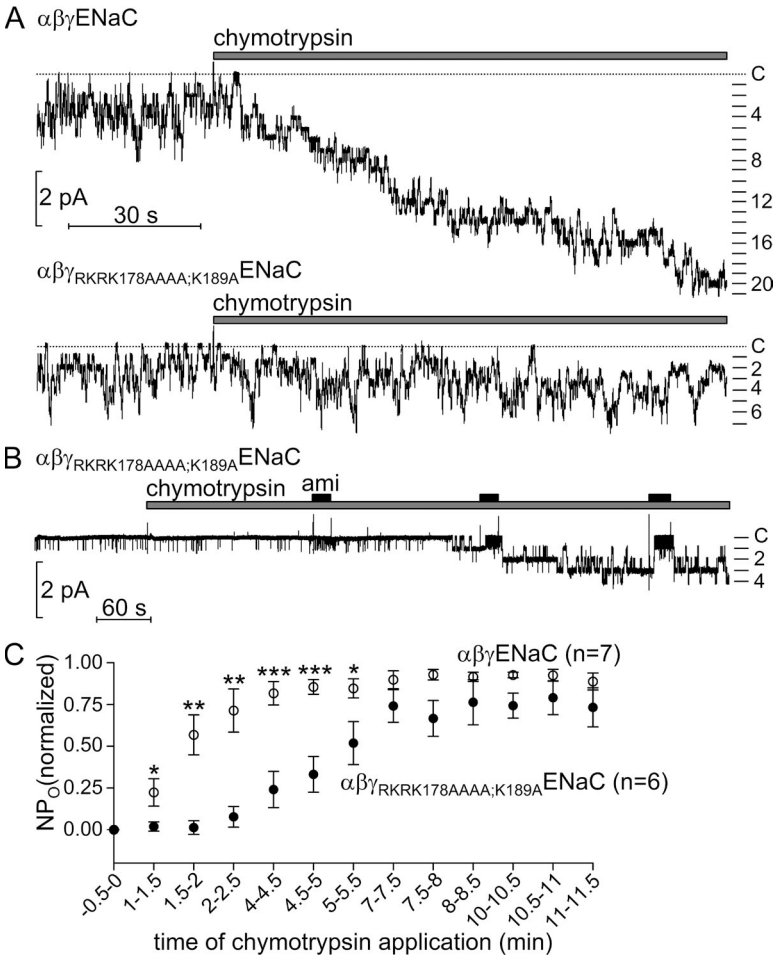

Figure 9. Delayed proteolytic activation of near-silent channels in outside-out patches from oocytes expressing the $\alpha\beta\gamma_{RKRK178AAAA;K189A}$ mutant channel. (A) Representative single-channel current recordings obtained at a holding potential of −70 mV from an outside-out patch of an oocyte expressing αβγ (top trace) or $\alpha\beta\gamma_{RKRK178AAAA;K189A}$ (bottom trace) ENaC. 2 μg/ml chymotrypsin was present in the bath solution, as indicated by the gray bar. The current level at which all channels are closed (C) is indicated by a dotted line. (B) The experiment was performed as described in A, obtained from an outside-out patch of an oocyte expressing $\alpha\beta\gamma_{RKRK178AAAA;K189A}$ mutant ENaC. 2 μM amiloride (ami) and 2 μg/ml chymotrypsin were applied as indicated by closed and gray bars, respectively. (C) Time course of the averaged normalized NP_O values after chymotrypsin application calculated from outside-out patch-clamp recordings as shown in A and B. In each individual experiment, NP_O values before the application of chymotrypsin were set to zero, and maximal NP_O values after chymotrypsin application were set to one. *, $P < 0.05$; **, $P < 0.01$; ***, $P < 0.001$; unpaired t test.

of chymotrypsin on ENaC (Fig. 10 A). In contrast, the stimulatory effect of trypsin was not different in oocytes expressing wt or $\alpha\beta\gamma_{FF174AA}$ mutant channel (Fig. 10 A). Basal ΔI_{ami} values of wt and $\gamma_{FF174AA}$ mutant–expressing oocytes were of similar size (Fig. S1 D). To study the effect of the $\gamma_{FF174AA}$ mutation on channel cleavage, we detected γENaC at the cell surface of wt and $\gamma_{FF174AA}$ENaC-expressing oocytes after preincubation in control, chymotrypsin, or trypsin solution (Fig. 10, B and C).

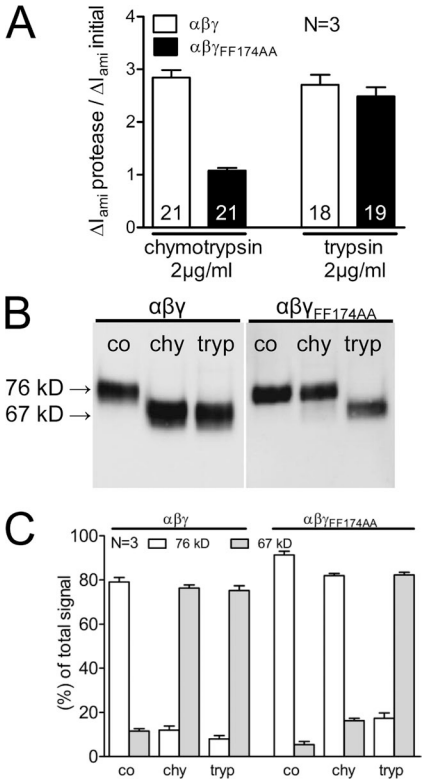

Figure 10. Mutating two phenylalanine residues (γFF174) adjacent to the prostasin cleavage site prevents proteolytic activation of ENaC by chymotrypsin. Continuous whole cell current measurements were performed in oocytes expressing αβγ or $\alpha\beta\gamma_{FF174AA}$ENaC. ΔI_{ami} was determined before and after superfusing the oocytes with 2 µg/ml chymotrypsin or 2 µg/ml trypsin (A). For biotinylation experiments, matched oocytes were preincubated for 30 min in protease-free solution (control) or in a solution containing either 2 µg/ml chymotrypsin or 2 µg/ml trypsin (B and C). In parallel to the detection of ΔI_{ami}, expression of biotinylated γENaC at the cell surface was analyzed by SDS-PAGE. γENaC was detected with an antibody against the C terminus of human γENaC. (A) Columns represent relative stimulatory effect on ΔI_{ami} calculated as the ratio of ΔI_{ami} after chymotrypsin/trypsin superfusion (ΔI_{ami} protease) to the initial ΔI_{ami} (ΔI_{ami} initial). (B) γENaC was detected with an antibody against the C terminus of human γENaC. Representative Western blots from oocytes expressing αβγ or $\alpha\beta\gamma_{FF174AA}$ENaC. In noninjected oocytes, γENaC-specific signals were absent (not depicted). (C) Densitometric analysis of four Western blots similar to those shown in B. For each lane, the signals detected in the regions of 76 kD (open columns) and 67 kD (gray columns) were determined and normalized to the sum of the total signal detected. *N* indicates the number of different batches of oocytes.

Detection of γENaC in untreated wt and $\gamma_{FF174AA}$ENaC-expressing control oocytes revealed a predominant band of 76 kD (Fig. 10 B). In wt ENaC–expressing oocytes, channel activation by chymotrypsin or trypsin led to the appearance of a 67-kD band (Fig. 10, B and C). In contrast, in $\gamma_{FF174AA}$ENaC-expressing oocytes, the 76-kD band remained the predominant band after exposure to chymotrypsin. However, treating the $\gamma_{FF174AA}$ mutant channel with trypsin resulted in the appearance of a 67-kD band (Fig. 10, B and C), which is consistent with the current activation observed with trypsin.

In summary, we have demonstrated that mutating the two phenylalanines (γFF174) is sufficient to prevent the stimulatory effect of chymotrypsin on proteolytic ENaC activation, whereas the stimulatory effect of trypsin on ENaC is preserved. These data suggest that the two phenylalanines constitute a preferential cleavage site for ENaC activation by chymotrypsin.

High concentrations of chymotrypsin can overcome the effect of the $\gamma_{FF174AA}$ mutation to prevent channel activation

As shown above (Fig. 10), the $\gamma_{FF174AA}$ mutation prevented ENaC activation by chymotrypsin (2 µg/ml for 30 min). We speculated that proteolytic activation of $\gamma_{FF174AA}$ENaC by chymotrypsin may be restored by using chymotrypsin in a higher concentration. Therefore, we performed additional experiments using 10 µg/ml chymotrypsin. As shown in Fig. 11 A (right), a 30-min exposure of oocytes expressing $\gamma_{FF174AA}$ENaC to 10 µg/ml resulted in a substantial ENaC stimulation. In contrast, in matched oocytes the $\gamma_{FF174AA}$ mutation prevented a stimulation by 2 µg/ml chymotrypsin (Fig. 11 A, left), consistent with the results shown in Fig. 10. In good agreement with these current data, an additional cleavage product of 67 kD only appeared in $\gamma_{FF174AA}$ENaC-expressing oocytes treated with 10 µg/ml chymotrypsin but not in those treated with 2 µg/ml chymotrypsin (Fig. 11, B and C). These results demonstrate that a high concentration of chymotrypsin can overcome the effect of the $\gamma_{FF174AA}$ mutation to prevent proteolytic channel activation. As expected, exposing wt ENaC–expressing oocytes to 2 or 10 µg/ml chymotrypsin activated ENaC currents and resulted in the disappearance of the 76-kD band and the appearance of a 67-kD band (Fig. 11, B and C).

To test the possibility that the stimulatory effect of 10 µg/ml chymotrypsin is mediated by one of the previously described cleavage sites in the vicinity of the γFF174 residues, we generated a mutant channel ($\gamma_{FF174AA;RKRK178AAAA;V182G;K189A;V193G}$) in which in addition to the two phenylalanines (FF174), the putative cleavage sites for prostasin (RKRK178), plasmin (K189), and neutrophil elastase (V182 and V193) were mutated. Basal ΔI_{ami} values of wt and $\gamma_{FF174AA;RKRK178AAAA;V182G;K189A;V193G}$

mutant–expressing oocytes were of similar size (Fig. S1 E). In oocytes expressing this mutant channel, 2 as well as 10 µg/ml chymotrypsin failed to activate ENaC currents and to generate a 67-kD cleavage product. In contrast, the $\gamma_{FF174AA;RKRK178AAAA;V182G;K189A;V193G}$ mutation did not prevent ENaC activation by trypsin (not depicted). The finding that a high concentration of chymotrypsin (10 µg/ml) can stimulate the $\gamma_{FF174AA}$ but not the $\gamma_{FF174AA;RKRK178AAAA;V182G;K189A;V193G}$ mutant channel supports the concept that under certain conditions, chymotrypsin may cleave at other sites in addition to its preferential cleavage at γFF174.

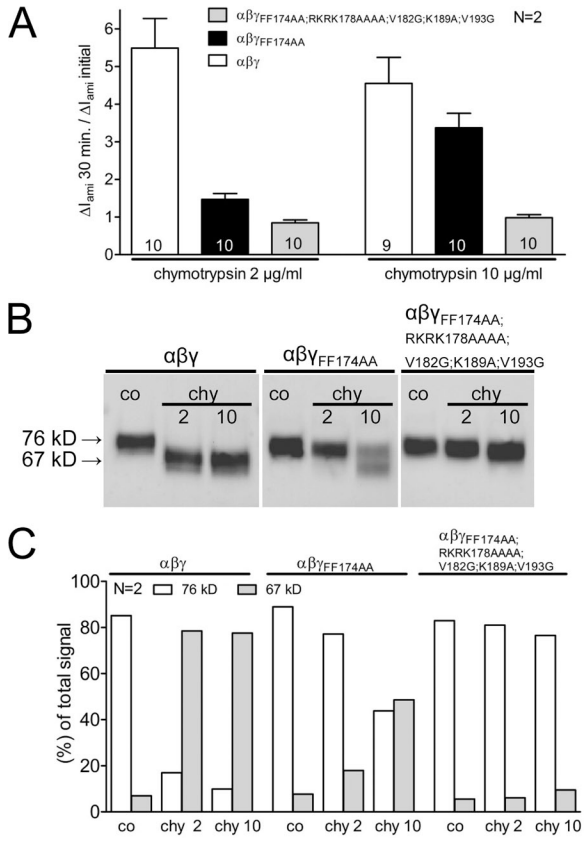

Figure 11. High concentrations of chymotrypsin can overcome the effect of the $\gamma_{FF174AA}$ mutation to prevent channel activation. Oocytes expressing αβγ, $\alpha\beta\gamma_{FF174AA}$, or $\alpha\beta\gamma_{FF174AA;RKRK178AAAA;V182G;K189A;V193G}$ ENaC were preincubated for 30 min in protease-free solution (control) or in a solution containing 2 or 10 µg/ml chymotrypsin. Amiloride-sensitive whole cell currents (ΔI_{ami}) were determined before and after incubation. In parallel to the detection of ΔI_{ami}, expression of biotinylated γENaC at the cell surface was analyzed by SDS-PAGE. γENaC was detected with an antibody against the C terminus of human γENaC. (A) Columns represent relative stimulatory effect on ΔI_{ami} calculated as the ratio of ΔI_{ami} measured after a 30-min preincubation (ΔI_{ami} 30 min) to the initial ΔI_{ami} (ΔI_{ami} initial) measured before incubation. Numbers inside the columns indicate the number of individual oocytes measured. *N* indicates the number of different batches of oocytes. (B) γENaC was detected with an antibody against the C terminus of human γENaC. Representative Western blots from oocytes expressing αβγ, $\alpha\beta\gamma_{FF174AA}$, or $\alpha\beta\gamma_{FF174AA;RKRK178AAAA;V182G;K189A;V193G}$ ENaC. In noninjected oocytes, γENaC-specific signals were absent (not depicted). (C) Densitometric analysis of two Western blots similar to those shown in B. For each lane, the signals detected in the regions of 76 kD (open columns) and 67 kD (gray columns) were determined and normalized to the sum of the total signal detected. *N* indicates the number of different batches of oocytes.

DISCUSSION

In this study, we identified two cleavage sites in the γ subunit of human ENaC with functional importance for its proteolytic activation by the protease plasmin. We demonstrated that mutating the putative plasmin cleavage site (K189) corresponding to the known plasmin cleavage site in mouse ENaC is not sufficient to abolish proteolytic activation of human ENaC by plasmin. Additional mutation of the putative prostasin site (RKRK178) was required to fully prevent channel activation by plasmin. These findings indicate that the K189 site is the preferential cleavage site for plasmin but that the RKRK178 prostasin site serves as an alternative cleavage site when the K189 site is not available. Interestingly, mutating these two sites also delayed channel activation by chymotrypsin. The delayed current activation of the double mutant channel by chymotrypsin was paralleled by a delayed appearance of a 67-kD γENaC cleavage product that corresponds to the fully cleaved subunit. To our knowledge, this is the first demonstration that the time course of proteolytic activation of ENaC-mediated whole cell currents correlates with the appearance of a γENaC cleavage product at the cell surface. Importantly, the γ subunit detected in the plasma membrane before proteolytic channel activation is already precleaved at the putative furin site, as indicated by the predominant presence of a 76-kD fragment instead of a full-length γ subunit with the expected size of ∼87 kD. Thus, our results confirm the concept that a second cleavage event in γENaC is required as a final step in proteolytic channel activation (Soundararajan et al., 2010; Kota et al., 2012). Moreover, we demonstrated that channel activation by chymotrypsin was prevented by mutating two phenylalanine residues (γFF174). This is the first report of a preferential cleavage site for chymotrypsin involved in ENaC activation.

The putative plasmin cleavage site in human γENaC (K189) was identified by sequence comparison with mouse γENaC. Plasmin preferentially cleaves after the basic residues lysine and arginine. Therefore, the residue K189 is a plausible cleavage site for plasmin. Mutating the putative plasmin cleavage site (K194) in mouse γENaC has been reported to abolish the stimulatory effect of plasmin on ENaC (Passero et al., 2008). We could confirm that 10 µg/ml plasmin failed to activate mouse ENaC with a mutated plasmin cleavage site (γ_{K194A}), even with an extended preincubation time of 30 min (Fig. S2). In contrast, mutating the corresponding site in human γENaC (K189A) reduced but did not

abolish the stimulatory effect of 10 μg/ml plasmin on ENaC. This indicates that in human ENaC, this site is a preferential site for cleavage by plasmin but not the only possible cleavage site for proteolytic ENaC activation by plasmin.

We also demonstrated that inactivation of the putative prostasin cleavage site ($\gamma_{RKRK178AAAA}$) per se had no effect on the activation of human ENaC by plasmin. This is in good agreement with findings reported for mouse ENaC (Passero et al., 2008). The preference of plasmin for the K189 site probably explains why mutating the prostasin site (RKRK178) does not affect activation of human ENaC by plasmin, whereas mutating the plasmin site (K189) reduces the activating effect of plasmin. We conclude that when the preferential plasmin cleavage site K189 is not available, plasmin may use the putative prostasin site (RKRK178) as an alternative cleavage site to activate human ENaC. The finding that mutating both sites abolishes the stimulatory effect of plasmin indicates that no other sites serve as plasmin cleavage sites in human γENaC.

Our results suggest that the mechanism of ENaC activation by plasmin differs between mouse and human, which highlights the importance and impact of subtle species differences in ion channel regulation. Interestingly, sequence inspection (Fig. 1) reveals that three corresponding amino acids in close vicinity of the putative prostasin cleavage site in γENaC are different in mouse and human (I187, S188, and K190 in mouse vs. V182, G183, and S185 in human). In particular, a putative cleavage site for human neutrophil elastase (V182) in human γENaC (Adebamiro et al., 2007) is not conserved in mouse γENaC (I187). Thus, these corresponding regions in human and mouse γENaC may well display different sensitivities to proteases. This may explain why the putative prostasin site can contribute to the activation of human ENaC by plasmin but probably not to that of mouse ENaC.

Serine protease specificity is defined by how substrates compete for an enzyme and is determined by complex mechanisms (Hedstrom, 2002). Proteases applied in high concentrations may target cleavage sites that they would not normally access under physiological conditions. However, we applied plasmin in the same concentration as reported by Passero et al. (2008) (10 μg/ml), which is in a range reported to be pathophysiologically relevant in PAN-nephrotic rats in an acute episode of proteinuria (Svenningsen et al., 2009b). Therefore, nonspecific cleavage is unlikely to explain the residual stimulatory effect of plasmin on human ENaC with a mutation of the putative plasmin site.

There is good evidence that detection of cleaved ENaC fragments is associated with states of high ENaC activity in native tissue (Ergonul et al., 2006; Frindt et al., 2008). However, until now, a time-dependent parallel increase in ENaC currents and cleavage products at the cell surface has not yet been reported. In this study, we demonstrated for the first time a clear correlation between ENaC current activation and the appearance of a 67-kD cleavage fragment of γENaC. We showed that proteolytic ENaC activation by chymotrypsin was slowed down in oocytes expressing the double mutant channel with mutations in the putative plasmin and prostasin cleavage sites. The slower increase in ENaC currents nicely correlated with the delayed appearance of γENaC cleavage products at the cell surface. This is an important finding because it indicates a causal link between cleavage and channel activation.

Using outside-out patches of oocytes expressing the double mutant ENaC, we confirmed the delayed onset of proteolytic activation of the double mutant channel at the single-channel level. We could show that the delayed activation of the double mutant channel by chymotrypsin was caused by a delayed stepwise recruitment of so-called near-silent channels. But how can we explain that the $\gamma_{RKRK178AAAA;K189A}$ mutation delays ENaC activation by chymotrypsin?

The amino acids phenylalanine, tyrosine, and tryptophan are preferential cleavage residues for chymotrypsin. Thus, neither RKRK178 nor K189 is a likely cleavage site for chymotrypsin. Instead of these sites, we identified two phenylalanine residues in γENaC (FF174) as likely cleavage sites for chymotrypsin. Indeed, we found that mutating γFF174 is sufficient to prevent the stimulatory effect of 2 μg/ml chymotrypsin on proteolytic ENaC activation. This indicates that γFF174 represents a preferential cleavage site for chymotrypsin. Interestingly, the prostasin cleavage site is located in close proximity to these two phenylalanine residues. Therefore, it is conceivable that mutating the prostasin cleavage site causes a sterical modification of the channel in this region. This may reduce the accessibility of chymotrypsin to its preferential cleavage sites (FF174). This hypothesis is consistent with our result that it is sufficient to mutate the prostasin cleavage site to delay ENaC activation by chymotrypsin.

The surprising finding that the stimulatory effect of chymotrypsin was not reduced but slightly increased in oocytes expressing ENaC with a mutated plasmin site may also be caused by a conformational change in the channel structure induced by the mutation. It is tempting to speculate that in this case the induced conformational change may improve the accessibility of chymotrypsin to its preferential cleavage site FF174.

In summary, our findings indicate that in addition to a putative plasmin site (K189), a putative prostasin cleavage site (RKRK178) may serve as an alternative cleavage site for proteolytic activation of human ENaC by plasmin. Plasmin preferentially activates the channel by cleaving it at the plasmin cleavage site. However, when the plasmin cleavage site is mutated, the prostasin site provides an alternative cleavage site for plasmin. This is

supported by the finding that both sites have to be mutated to abolish proteolytic ENaC activation by plasmin. Furthermore, we clearly demonstrate that proteolytic current activation is paralleled by the appearance of a 67-kD proteolytic γENaC fragment at the cell surface. This provides evidence for a causal link between proteolytic cleavage and channel activation. In addition, we identified for the first time a preferential cleavage site for chymotrypsin (γFF174). The close proximity of the prostasin site to the FF174 site probably explains why mutating the prostasin site causes a delay in channel activation by chymotrypsin. The fact that γENaC contains several different cleavage sites in a region critical for proteolytic channel activation is likely to have physiological implications. Indeed, it may provide a mechanism for differential ENaC regulation by tissue-specific proteases.

The expert technical assistance of Céline Grüninger, Sonja Mayer, Jessica Rinke, and Ralf Rinke is gratefully acknowledged.

This study was supported by grants of the Interdisziplinäres Zentrum für Klinische Forschung (to S. Haerteis and M. Krappitz) and the ELAN program (to S. Haerteis) of the Friedrich-Alexander-Universität Erlangen-Nürnberg.

Lawrence G. Palmer served as editor.

Submitted: 23 December 2011
Accepted: 20 August 2012

REFERENCES

Adebamiro, A., Y. Cheng, U.S. Rao, H. Danahay, and R.J. Bridges. 2007. A segment of γ ENaC mediates elastase activation of Na^+ transport. *J. Gen. Physiol.* 130:611–629. http://dx.doi.org/10.1085/jgp.200709781

Bruns, J.B., M.D. Carattino, S. Sheng, A.B. Maarouf, O.A. Weisz, J.M. Pilewski, R.P. Hughey, and T.R. Kleyman. 2007. Epithelial Na^+ channels are fully activated by furin- and prostasin-dependent release of an inhibitory peptide from the γ-subunit. *J. Biol. Chem.* 282:6153–6160. http://dx.doi.org/10.1074/jbc.M610636200

Caldwell, R.A., R.C. Boucher, and M.J. Stutts. 2004. Serine protease activation of near-silent epithelial Na^+ channels. *Am. J. Physiol. Cell Physiol.* 286:C190–C194. http://dx.doi.org/10.1152/ajpcell.00342.2003

Caldwell, R.A., R.C. Boucher, and M.J. Stutts. 2005. Neutrophil elastase activates near-silent epithelial Na^+ channels and increases airway epithelial Na^+ transport. *Am. J. Physiol. Lung Cell. Mol. Physiol.* 288:L813–L819. http://dx.doi.org/10.1152/ajplung.00435.2004

Canessa, C.M. 2007. Structural biology: unexpected opening. *Nature.* 449:293–294. http://dx.doi.org/10.1038/449293a

Carattino, M.D., R.P. Hughey, and T.R. Kleyman. 2008. Proteolytic processing of the epithelial sodium channel γ subunit has a dominant role in channel activation. *J. Biol. Chem.* 283:25290–25295. http://dx.doi.org/10.1074/jbc.M803931200

Chraïbi, A., V. Vallet, D. Firsov, S.K. Hess, and J.D. Horisberger. 1998. Protease modulation of the activity of the epithelial sodium channel expressed in *Xenopus* oocytes. *J. Gen. Physiol.* 111:127–138. http://dx.doi.org/10.1085/jgp.111.1.127

Diakov, A., and C. Korbmacher. 2004. A novel pathway of epithelial sodium channel activation involves a serum- and glucocorticoid-inducible kinase consensus motif in the C terminus of the channel's α-subunit. *J. Biol. Chem.* 279:38134–38142. http://dx.doi.org/10.1074/jbc.M403260200

Diakov, A., K. Bera, M. Mokrushina, B. Krueger, and C. Korbmacher. 2008. Cleavage in the γ-subunit of the epithelial sodium channel (ENaC) plays an important role in the proteolytic activation of near-silent channels. *J. Physiol.* 586:4587–4608. http://dx.doi.org/10.1113/jphysiol.2008.154435

Ergonul, Z., G. Frindt, and L.G. Palmer. 2006. Regulation of maturation and processing of ENaC subunits in the rat kidney. *Am. J. Physiol. Renal Physiol.* 291:F683–F693. http://dx.doi.org/10.1152/ajprenal.00422.2005

Firsov, D., L. Schild, I. Gautschi, A.M. Mérillat, E. Schneeberger, and B.C. Rossier. 1996. Cell surface expression of the epithelial Na channel and a mutant causing Liddle syndrome: a quantitative approach. *Proc. Natl. Acad. Sci. USA.* 93:15370–15375. http://dx.doi.org/10.1073/pnas.93.26.15370

Firth, J.D., E.S. Sue, E.E. Putnins, D. Oda, and V.J. Uitto. 1996. Chymotrypsin-like enzyme secretion is stimulated in cultured epithelial cells during proliferation and in response to Actinobacillus actinomycetemcomitans. *J. Periodontal Res.* 31:345–354. http://dx.doi.org/10.1111/j.1600-0765.1996.tb00502.x

Frindt, G., Z. Ergonul, and L.G. Palmer. 2008. Surface expression of epithelial Na channel protein in rat kidney. *J. Gen. Physiol.* 131:617–627. http://dx.doi.org/10.1085/jgp.200809989

Haerteis, S., B. Krueger, C. Korbmacher, and R. Rauh. 2009. The δ-subunit of the epithelial sodium channel (ENaC) enhances channel activity and alters proteolytic ENaC activation. *J. Biol. Chem.* 284:29024–29040. http://dx.doi.org/10.1074/jbc.M109.018945

Haerteis, S., D. Schaal, F. Brauer, S. Brüschke, K. Schweimer, R. Rauh, H. Sticht, P. Rösch, S. Schwarzinger, and C. Korbmacher. 2012. An inhibitory peptide derived from the α-subunit of the epithelial sodium channel (ENaC) shows a helical conformation. *Cell. Physiol. Biochem.* 29:761–774.

Harris, M., D. Firsov, G. Vuagniaux, M.J. Stutts, and B.C. Rossier. 2007. A novel neutrophil elastase inhibitor prevents elastase activation and surface cleavage of the epithelial sodium channel expressed in *Xenopus laevis* oocytes. *J. Biol. Chem.* 282:58–64. http://dx.doi.org/10.1074/jbc.M605125200

Harris, M., A. Garcia-Caballero, M.J. Stutts, D. Firsov, and B.C. Rossier. 2008. Preferential assembly of epithelial sodium channel (ENaC) subunits in *Xenopus* oocytes: role of furin-mediated endogenous proteolysis. *J. Biol. Chem.* 283:7455–7463. http://dx.doi.org/10.1074/jbc.M707399200

Hedstrom, L. 2002. Serine protease mechanism and specificity. *Chem. Rev.* 102:4501–4524. http://dx.doi.org/10.1021/cr000033x

Hughey, R.P., J.B. Bruns, C.L. Kinlough, K.L. Harkleroad, Q. Tong, M.D. Carattino, J.P. Johnson, J.D. Stockand, and T.R. Kleyman. 2004. Epithelial sodium channels are activated by furin-dependent proteolysis. *J. Biol. Chem.* 279:18111–18114. http://dx.doi.org/10.1074/jbc.C400080200

Hughey, R.P., M.D. Carattino, and T.R. Kleyman. 2007. Role of proteolysis in the activation of epithelial sodium channels. *Curr. Opin. Nephrol. Hypertens.* 16:444–450. http://dx.doi.org/10.1097/MNH.0b013e32821f6072

Jasti, J., H. Furukawa, E.B. Gonzales, and E. Gouaux. 2007. Structure of acid-sensing ion channel 1 at 1.9 Å resolution and low pH. *Nature.* 449:316–323. http://dx.doi.org/10.1038/nature06163

Ji, H.L., and D.J. Benos. 2004. Degenerin sites mediate proton activation of δβγ-epithelial sodium channel. *J. Biol. Chem.* 279:26939–26947. http://dx.doi.org/10.1074/jbc.M401143200

Kashlan, O.B., B.M. Blobner, Z. Zuzek, M.D. Carattino, and T.R. Kleyman. 2012. Inhibitory tract traps the epithelial Na^+ channel in a low activity conformation. *J. Biol. Chem.* 287:20720–20726. http://dx.doi.org/10.1074/jbc.M112.358218

Kleyman, T.R., and R.P. Hughey. 2009. Plasmin and sodium retention in nephrotic syndrome. *J. Am. Soc. Nephrol.* 20:233–234. http://dx.doi.org/10.1681/ASN.2008121236

Kleyman, T.R., M.D. Carattino, and R.P. Hughey. 2009. ENaC at the cutting edge: regulation of epithelial sodium channels by proteases. *J. Biol. Chem.* 284:20447–20451. http://dx.doi.org/10.1074/jbc.R800083200

Korbmacher, C., T. Volk, A.S. Segal, E.L. Boulpaep, and E. Frömter. 1995. A calcium-activated and nucleotide-sensitive nonselective cation channel in M-1 mouse cortical collecting duct cells. *J. Membr. Biol.* 146:29–45.

Koshikawa, N., S. Hasegawa, Y. Nagashima, K. Mitsuhashi, Y. Tsubota, S. Miyata, Y. Miyagi, H. Yasumitsu, and K. Miyazaki. 1998. Expression of trypsin by epithelial cells of various tissues, leukocytes, and neurons in human and mouse. *Am. J. Pathol.* 153:937–944. http://dx.doi.org/10.1016/S0002-9440(10)65635-0

Kota, P., A. García-Caballero, H. Dang, M. Gentzsch, M.J. Stutts, and N.V. Dokholyan. 2012. Energetic and structural basis for activation of the epithelial sodium channel by matriptase. *Biochemistry.* 51:3460–3469.

Krueger, B., S. Haerteis, L. Yang, A. Hartner, R. Rauh, C. Korbmacher, and A. Diakov. 2009. Cholesterol depletion of the plasma membrane prevents activation of the epithelial sodium channel (ENaC) by SGK1. *Cell. Physiol. Biochem.* 24:605–618. http://dx.doi.org/10.1159/000257516

Loffing, J., and C. Korbmacher. 2009. Regulated sodium transport in the renal connecting tubule (CNT) via the epithelial sodium channel (ENaC). *Pflugers Arch.* 458:111–135. http://dx.doi.org/10.1007/s00424-009-0656-0

Nesterov, V., A. Dahlmann, M. Bertog, and C. Korbmacher. 2008. Trypsin can activate the epithelial sodium channel (ENaC) in microdissected mouse distal nephron. *Am. J. Physiol. Renal Physiol.* 295:F1052–F1062. http://dx.doi.org/10.1152/ajprenal.00031.2008

Passero, C.J., G.M. Mueller, H. Rondon-Berrios, S.P. Tofovic, R.P. Hughey, and T.R. Kleyman. 2008. Plasmin activates epithelial Na^+ channels by cleaving the γ subunit. *J. Biol. Chem.* 283:36586–36591. http://dx.doi.org/10.1074/jbc.M805676200

Passero, C.J., R.P. Hughey, and T.R. Kleyman. 2010. New role for plasmin in sodium homeostasis. *Curr. Opin. Nephrol. Hypertens.* 19:13–19. http://dx.doi.org/10.1097/MNH.0b013e3283330fb2

Patel, A.B., J. Chao, and L.G. Palmer. 2012. Tissue kallikrein activation of the epithelial Na channel. *Am. J. Physiol. Renal Physiol.* 303:F540–F550. http://dx.doi.org/10.1152/ajprenal.00133.2012

Piedagnel, R., Y. Tiger, B. Lelongt, and P.M. Ronco. 2006. Urokinase (u-PA) is produced by collecting duct principal cells and is post-transcriptionally regulated by SV40 large-T, arginine vasopressin, and epidermal growth factor. *J. Cell. Physiol.* 206:394–401. http://dx.doi.org/10.1002/jcp.20485

Planès, C., and G.H. Caughey. 2007. Regulation of the epithelial Na^+ channel by peptidases. *Curr. Top. Dev. Biol.* 78:23–46. http://dx.doi.org/10.1016/S0070-2153(06)78002-4

Rauh, R., A. Diakov, A. Tzschoppe, J. Korbmacher, A.K. Azad, H. Cuppens, J.J. Cassiman, J. Dötsch, H. Sticht, and C. Korbmacher. 2010. A mutation of the epithelial sodium channel associated with atypical cystic fibrosis increases channel open probability and reduces Na^+ self inhibition. *J. Physiol.* 588:1211–1225. http://dx.doi.org/10.1113/jphysiol.2009.180224

Rossier, B.C. 2002. Hormonal regulation of the epithelial sodium channel ENaC: N or P_o? *J. Gen. Physiol.* 120:67–70. http://dx.doi.org/10.1085/jgp.20028638

Rossier, B.C., and L. Schild. 2008. Epithelial sodium channel: mendelian versus essential hypertension. *Hypertension.* 52:595–600. http://dx.doi.org/10.1161/HYPERTENSIONAHA.107.097147

Rossier, B.C., and M.J. Stutts. 2009. Activation of the epithelial sodium channel (ENaC) by serine proteases. *Annu. Rev. Physiol.* 71:361–379. http://dx.doi.org/10.1146/annurev.physiol.010908.163108

Soundararajan, R., D. Pearce, R.P. Hughey, and T.R. Kleyman. 2010. Role of epithelial sodium channels and their regulators in hypertension. *J. Biol. Chem.* 285:30363–30369. http://dx.doi.org/10.1074/jbc.R110.155341

Stewart, A.P., S. Haerteis, A. Diakov, C. Korbmacher, and J.M. Edwardson. 2011. Atomic force microscopy reveals the architecture of the epithelial sodium channel (ENaC). *J. Biol. Chem.* 286:31944–31952. http://dx.doi.org/10.1074/jbc.M111.275289

Stockand, J.D., A. Staruschenko, O. Pochynyuk, R.E. Booth, and D.U. Silverthorn. 2008. Insight toward epithelial Na^+ channel mechanism revealed by the acid-sensing ion channel 1 structure. *IUBMB Life.* 60:620–628. http://dx.doi.org/10.1002/iub.89

Svenningsen, P., C. Bistrup, U.G. Friis, M. Bertog, S. Haerteis, B. Krueger, J. Stubbe, O.N. Jensen, H.C. Thiesson, T.R. Uhrenholt, et al. 2009a. Plasmin in nephrotic urine activates the epithelial sodium channel. *J. Am. Soc. Nephrol.* 20:299–310. http://dx.doi.org/10.1681/ASN.2008040364

Svenningsen, P., T.R. Uhrenholt, Y. Palarasah, K. Skjødt, B.L. Jensen, and O. Skøtt. 2009b. Prostasin-dependent activation of epithelial Na^+ channels by low plasmin concentrations. *Am. J. Physiol. Regul. Integr. Comp. Physiol.* 297:R1733–R1741. http://dx.doi.org/10.1152/ajpregu.00321.2009

Svenningsen, P., U.G. Friis, C. Bistrup, K.B. Buhl, B.L. Jensen, and O. Skøtt. 2011. Physiological regulation of epithelial sodium channel by proteolysis. *Curr. Opin. Nephrol. Hypertens.* 20:529–533. http://dx.doi.org/10.1097/MNH.0b013e328348bcc7

Svenningsen, P., O. Skøtt, and B.L. Jensen. 2012. Proteinuric diseases with sodium retention: Is plasmin the link? *Clin. Exp. Pharmacol. Physiol.* 39:117–124. http://dx.doi.org/10.1111/j.1440-1681.2011.05524.x

Vaziri, N.D., E.C. Gonzales, B. Shayestehfar, and C.H. Barton. 1994. Plasma levels and urinary excretion of fibrinolytic and protease inhibitory proteins in nephrotic syndrome. *J. Lab. Clin. Med.* 124:118–124.

Waldmann, R., G. Champigny, F. Bassilana, N. Voilley, and M. Lazdunski. 1995. Molecular cloning and functional expression of a novel amiloride-sensitive Na^+ channel. *J. Biol. Chem.* 270:27411–27414. http://dx.doi.org/10.1074/jbc.270.46.27411

Yamamura, H., S. Ugawa, T. Ueda, M. Nagao, and S. Shimada. 2004. Protons activate the δ-subunit of the epithelial Na^+ channel in humans. *J. Biol. Chem.* 279:12529–12534. http://dx.doi.org/10.1074/jbc.M400274200